

Development of a mesoscopic simulation method for atmospheric convection

Lian-Ping Wang¹, Wojciech W. Grabowski², Zhaoli Guo³, and Ryo Onishi⁴

¹Department of Mechanical Engineering, University of Delaware, USA

²Japan Agency for Marine-Earth Science and Technology, Japan

³National Center for Atmospheric Division, USA

⁴Huazhong University of Science and Technology, China

lwang@udel.edu

10:50 – 11:10, December 1 (Thursday)

The 4th International Workshop on Nonhydrostatic Models

Nov. 30 (Wed) - Dec. 2 (Fri), 2016

The Prince Hakone Lake Ashinoko, Hakone, Japan

Outline

- ❖ Background, motivation, and objectives
- ❖ The DUGKS method
- ❖ Some results
- ❖ Summary

Background & Motivation

- ✧ Mesoscopic methods based on the Boltzmann equation to solve complex turbulent flows have been rapidly developed over the last 30 years
- ✧ But very limited applications to geophysical flows

Overall objectives

- ✧ Simulate high-Rayleigh number convection flows using DUGKS
- ✧ How to treat unresolved local gradients?
 - Controlled local numerical diffusion (TVD, monotone,)
 - Explicit SGS model
- ✧ Compare DUGKS and Navier-Stokes based solvers in terms of accuracy, numerical stability, and efficiency

Thermal convection flows

Macroscopic world

$$\frac{\partial \rho}{\partial t} + \frac{\partial}{\partial x_j} (\rho u_j) = 0$$

$$\frac{\partial u_i}{\partial t} + u_j \frac{\partial u_i}{\partial x_j} = -\frac{1}{\bar{\rho}} \frac{\partial \tilde{p}}{\partial x_i} + \beta g (\theta - \theta_0) \delta_{i3} + \nu \frac{\partial^2 u_i}{\partial x_j \partial x_j}$$

$$\frac{\partial \theta}{\partial t} + \frac{\partial}{\partial x_j} (u_j \theta) = \frac{\partial}{\partial x_i} \left(\kappa \frac{\partial \theta}{\partial x_i} \right)$$

$$\theta = T - \bar{T}$$

Mesoscopic world

$$\partial_i f + \xi \cdot \nabla f = \tilde{\Omega} \equiv -\frac{f - f^{eq}}{\tau_v} + \Phi, \quad \Phi_i \approx \frac{\beta \vec{g} \theta \cdot (\vec{e}_i - \vec{u})}{RT} f_i^{(eq)}$$

$$\partial_i h + \xi \cdot \nabla h = \Psi \equiv -\frac{h - h^{eq}}{\tau_c}, \quad \theta = \sum_i h_i$$

$$\rho = \sum_i h_i, \quad \rho \vec{u} = \sum_i f_i \xi_i + \frac{\delta t}{2} \rho \beta \vec{g} \theta, \quad p = \rho R \theta$$

$$f^{eq} = \rho w_i \left[1 + \frac{\vec{e}_i \cdot \vec{u}}{c_s^2} + \frac{(\vec{e}_i \cdot \vec{u})^2}{2c_s^4} - \frac{\vec{u} \cdot \vec{u}}{2c_s^2} \right], \quad h^{eq} = \theta w_i \left[1 + \frac{\vec{e}_i \cdot \vec{u}}{c_s^2} + \frac{(\vec{e}_i \cdot \vec{u})^2}{2c_s^4} - \frac{\vec{u} \cdot \vec{u}}{2c_s^2} \right]$$

$$u_0 = \sqrt{g \beta \Delta T H}$$

$$Ra = \frac{g \beta \Delta T H^3}{\nu \kappa}$$

$$Pr = \frac{\nu}{\kappa} = 0.71$$

DUGKS: Discrete Unified Gas Kinetic Scheme

- ✧ Based directly on the Boltzmann equation with BGK collision model
- ✧ Gas Kinetic Scheme combined with certain good features of LBM (simplicity and low numerical dissipation)
- ✧ The kinetic advection is treated as fluxes through cell interfaces
- ✧ Fluxes are computed using distributions at the half time step, with streaming and collision coupled together (low numerical dissipation)
- ✧ A much more general approach than LBM
 - Key advantages: all flow types, all Kn and Ma
 - Non-uniform grid

K Xu and J-C Huang, *J. Comp. Phys.* 229, 7747 (2011)

ZL Guo, K Xu, RJ Wang, *PRE* 88, 033305 (2013); *PRE* 91, 033313 (2015)

P Wang, S Tao, ZL Guo, *Computers & Fluids*, 120 70-81 (2015).

DUGKS: finite-volume discretization for hydrodynamic velocity

$$\partial_t f + \xi \cdot \nabla f = \tilde{\Omega} \equiv -\frac{f - f^{eq}}{\tau_v} + \Phi$$

$$\xi \rightarrow \mathbf{e}_i, \quad \Phi_i \approx \frac{\beta \bar{g} (T - \bar{T}) \cdot (\bar{\mathbf{e}}_i - \bar{\mathbf{u}})}{RT} f_i^{(eq)}$$

For nearly incompressible flow, D3Q19

Updating rule for cell-center distribution functions

$$f_i^{n+1}(\mathbf{x}) - f_i^n(\mathbf{x}) + \underbrace{\frac{dt}{|V_j|} \sum_{dS} f_i^{n+0.5}(\mathbf{x}_s) \mathbf{e}_i \cdot dS}_{\text{Mid-point}} = \underbrace{\frac{dt}{2} [\tilde{\Omega}_i^{n+1} + \tilde{\Omega}_i^n]}_{\text{Trapezoidal}}$$

Mid-point

Trapezoidal

Constructing $f_i^{n+0.5}(\mathbf{x}_s)$: Integrate from t_n to $t_n + 0.5dt$ along the characteristic path

$$f_i^{n+0.5}(\mathbf{x}_s) - f_i^n(\mathbf{x}_s - 0.5dt \mathbf{e}_i) = \frac{dt}{4} [\tilde{\Omega}_i^{n+0.5}(\mathbf{x}_s) + \tilde{\Omega}_i^n(\mathbf{x}_s - 0.5dt \mathbf{e}_i)]$$

\mathbf{x} = cell center, \mathbf{x}_s = cell boundary

Similar transformations as in LBM are used to make all explicit

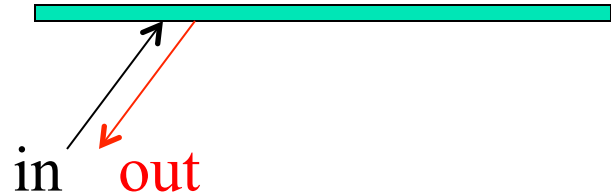
K Xu and J-C Huang, J. Comp. Phys. 229, 7747 (2011)

ZL Guo, K Xu, RJ Wang, PRE 88, 033305 (2013); PRE 91, 033313 (2015)

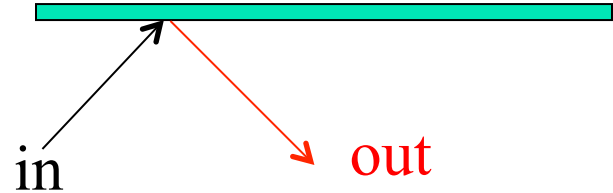
DUGKS: Boundary conditions

– all done to distributions at cell interfaces

No-slip wall: bounce-back



Free-slip wall: mirror reflection



Fixed temperature

$$h_{\bar{\alpha}}^{n+0.5}(\mathbf{x}_s) = -h_{\alpha}^{n+0.5}(\mathbf{x}_s) + 2W_{\alpha}T_{wall}$$

Zero heat flux

$$h_{\bar{\alpha}}^{n+0.5}(\mathbf{x}_s) = h_{\alpha}^{n+0.5}(\mathbf{x}_s)$$

DNS of turbulent flows using DUGKS

Homogeneous isotropic turbulence in a periodic box

Wang P, Wang L-P, Guo ZL, 2016, Comparison of the LBE and DUGKS methods for DNS of decaying turbulent flows. *Phys. Rev. E.*, 94, 043304

Turbulent channel flow [non-uniform mesh with large grid aspect ratios]

Bo YT, Wang P, Guo ZL, Wang L-P, 2016, Parallel implementation and validation of DUGKS for three-dimensional Taylor-Green vortex flow and turbulent channel flow, *Computers & Fluids*, *submitted*.

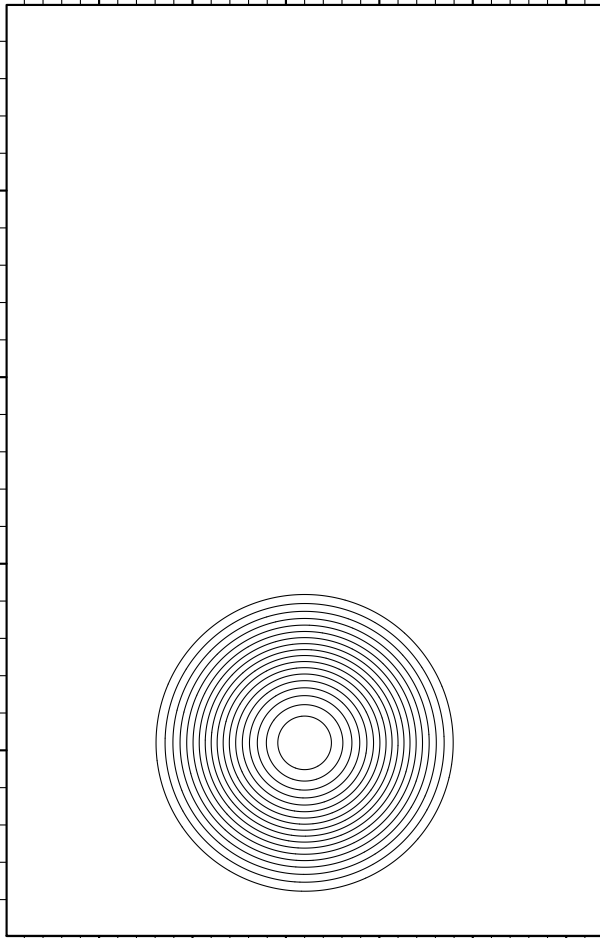
DNS of thermal convection in an enclosure

Wang L-P, Wen X, Geneva N, Wang P, Guo ZL, 2016, Simulations of high-Rayleigh-number convection flows using mesoscopic methods, *Discrete Simulation of Fluid Dynamics 2016*.

$Ra \sim 10^{11}$ in 3D

MPI, non-uniform mesh, external forcing, boundary conditions

The physical problem: Rising and evolution of a warm dry bubble



Background

$$\rho_0 = 1.0, \quad \theta_0 = 300K, \quad \Delta T = 2 \text{ K}$$

$$\theta = \theta_0 + \begin{cases} \Delta T \left[\cos\left(\frac{\pi r}{2000}\right) \right]^2 & r < 1000 \text{ m} \\ 0, & \text{otherwise} \end{cases}$$

Centered at 1040 m height

Domain: 3200 m H, 5000m V

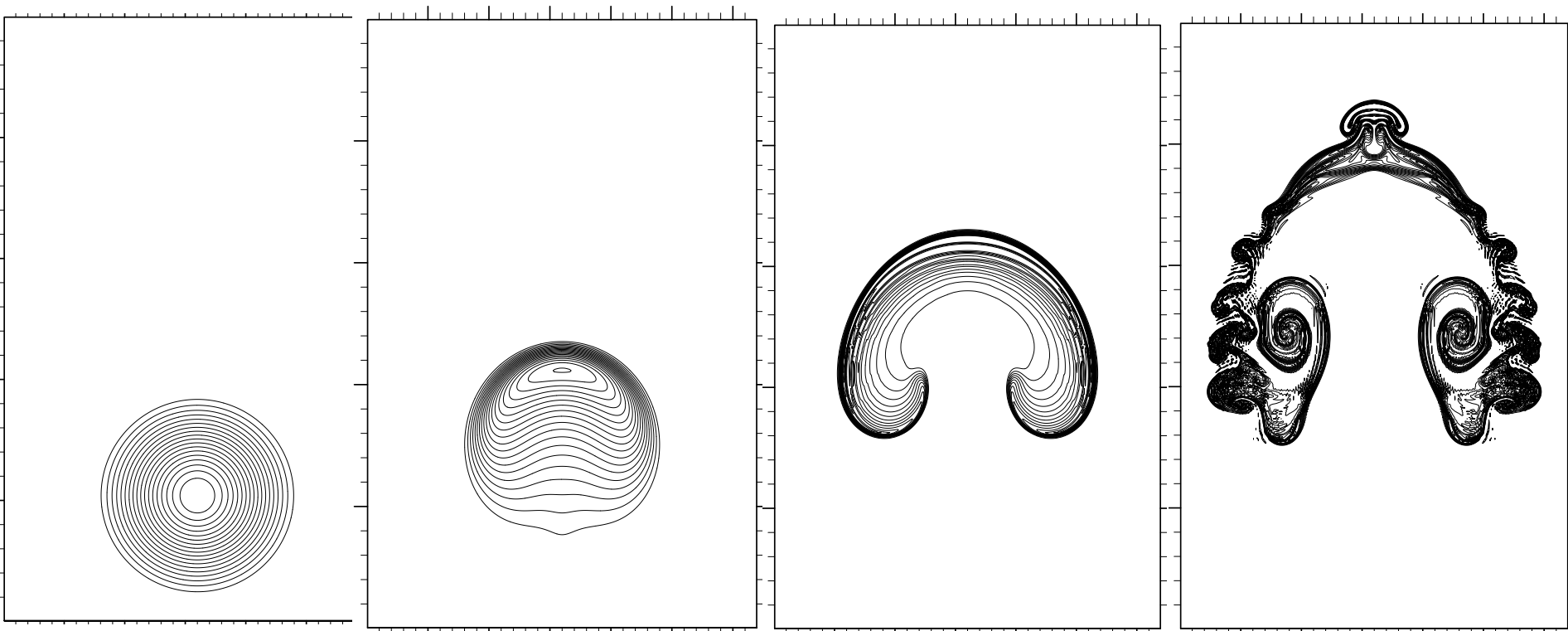
$$H = 1000 \text{ m}, \quad \text{Pr} = 0.71, \quad \nu = 1.57 \times 10^{-5}$$

$$Ra = \frac{\text{Pr} G \Delta T H^3}{\nu^2} = 1.89 \times 10^{17}$$

Periodic BC in horizontal

Vertical boundaries: zero heat flux & stress free

Evolution at a given grid resolution of $dx = 10$ m
No numerical limiter applied



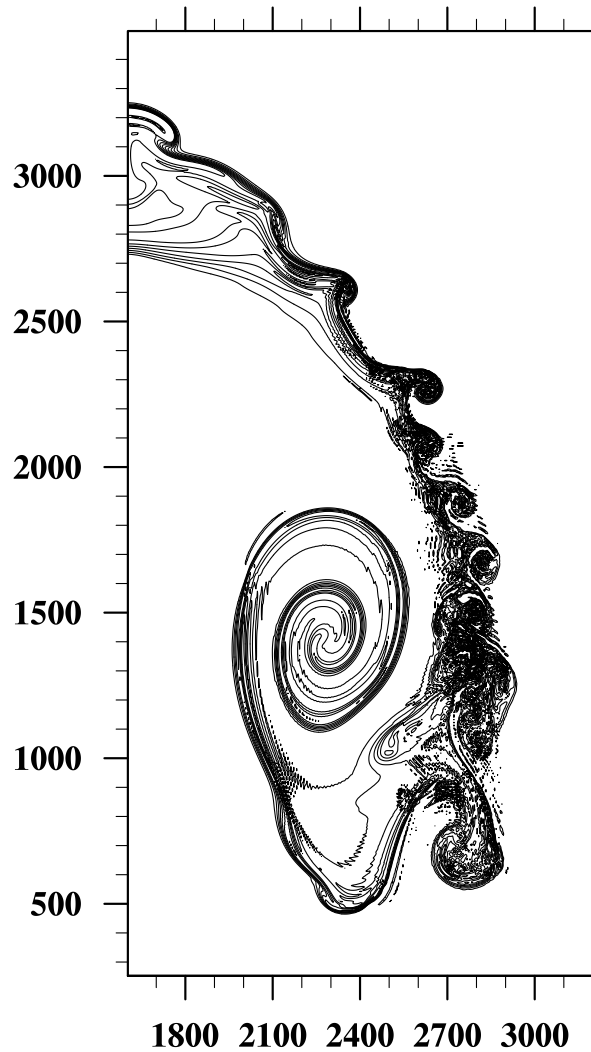
0 min

5 min

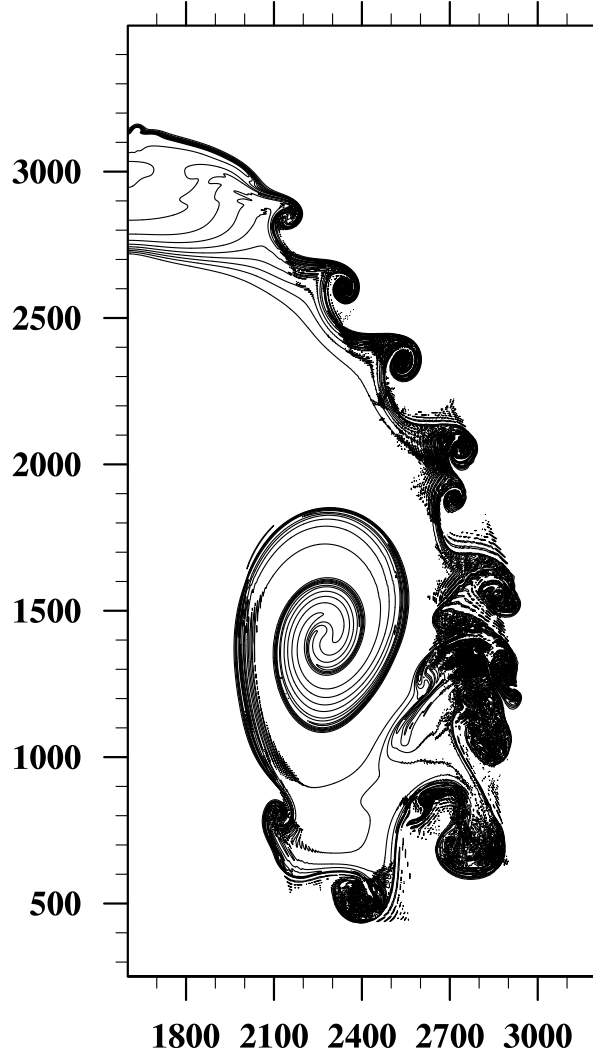
10 min

15 min

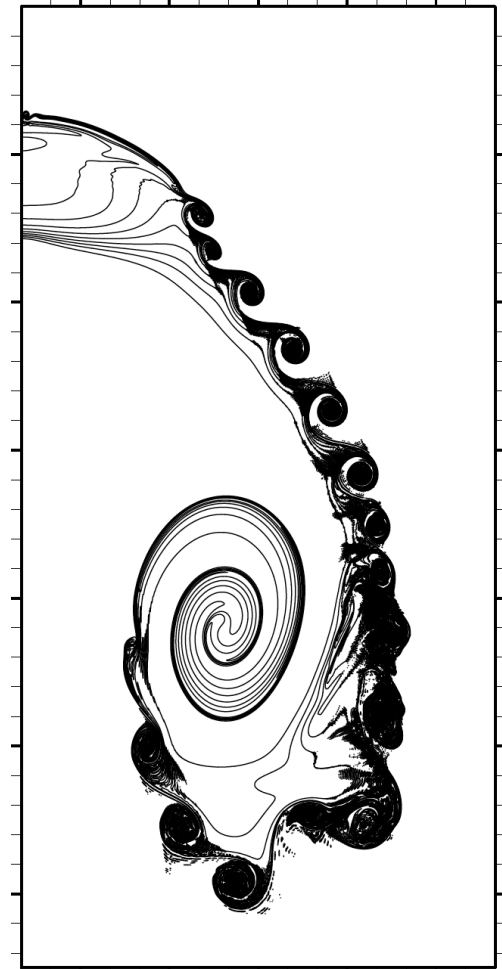
How about increasing the grid resolution? No numerical limiter applied



$dx=5.0$ m



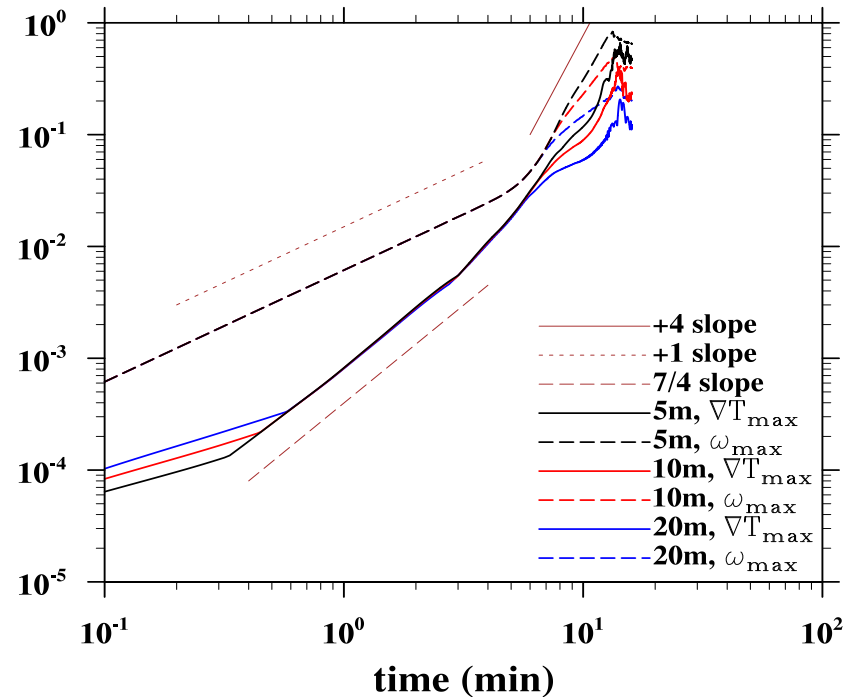
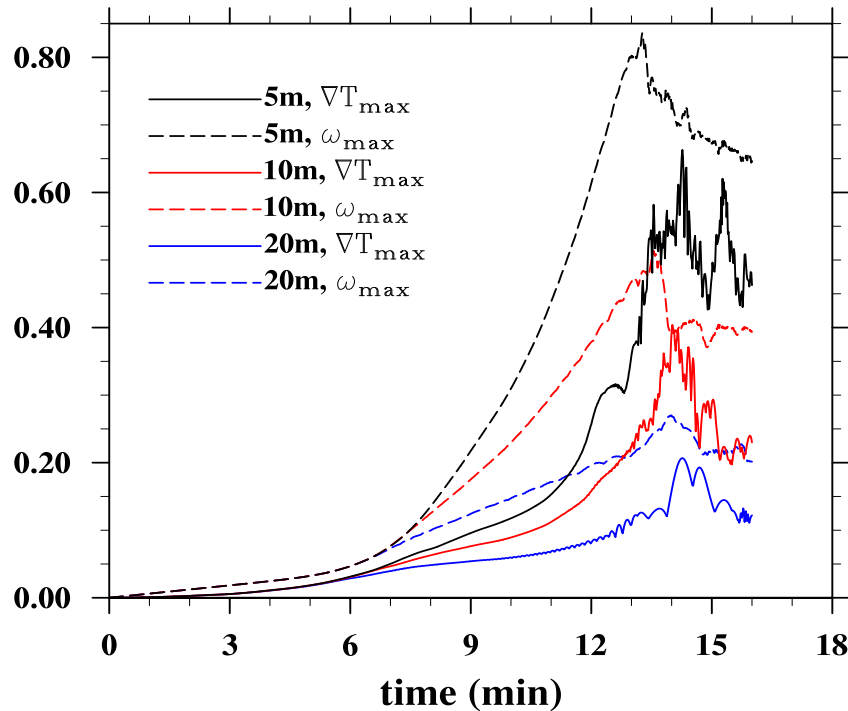
$dx=2.5$ m



$dx=1.25$ m

Maximum local temperature gradient and maximum local vorticity

→ Rapid evolution of the smallest spatial scale



- The higher the resolution, the more rapid the smallest scale is formed

The van-Leer slope limiter (the monotonized central limiter)

Slope in a cell for field reconstruction

$$\sigma_j^n = \text{minmod} \left(2 \frac{U_{j+1}^n - U_j^n}{\Delta x}, \frac{U_{j+1}^n - U_{j-1}^n}{2\Delta x}, 2 \frac{U_j^n - U_{j-1}^n}{\Delta x} \right) \quad (\text{Form 1})$$

where

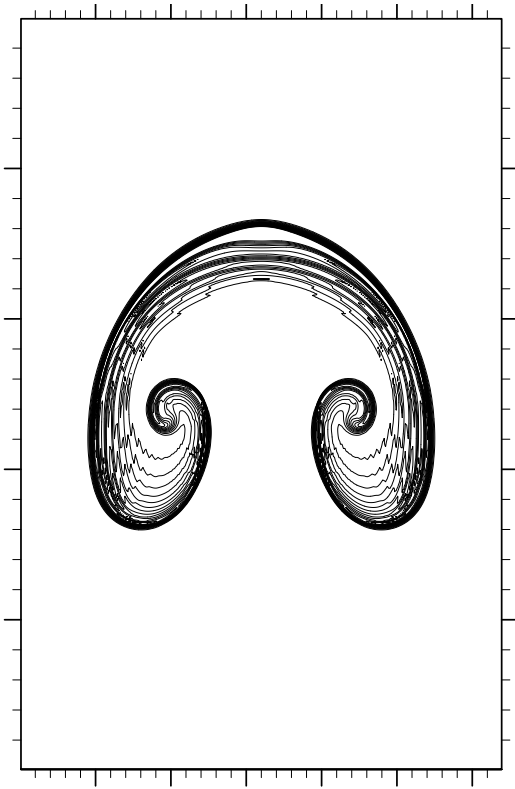
$$\text{minmod}(a_1, a_2, a_3) = \begin{cases} \text{sign}(a_1) \min(|a_1|, |a_2|, |a_3|), & \text{if } \text{sgn}(a_1) = \text{sgn}(a_2) = \text{sgn}(a_3) \\ 0, & \text{otherwise} \end{cases}$$

(Form 2)

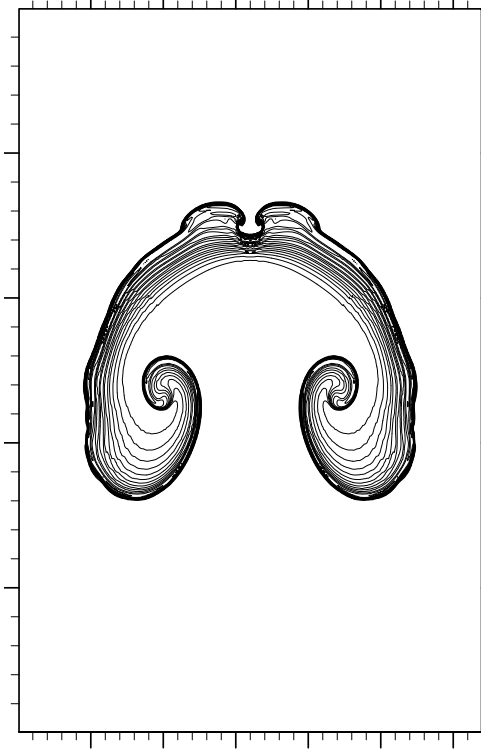
Variation

$$\sigma_j^n = \left[\text{sgn}(s_1) + \text{sgn}(s_2) \right] \frac{|s_1| |s_2|}{|s_1| + |s_2|}, \quad \text{where } s_1 = \frac{U_{j+1}^n - U_j^n}{\Delta x}, \quad s_2 = \frac{U_j^n - U_{j-1}^n}{\Delta x}$$

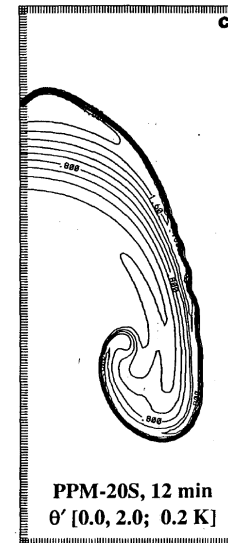
Time = 12.0 min, $dx = 10$ m, comparison of T field



No limiter



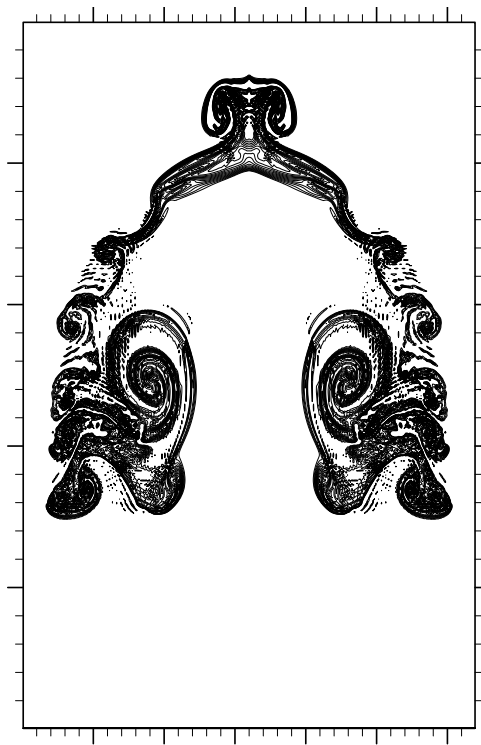
van Leer limiter



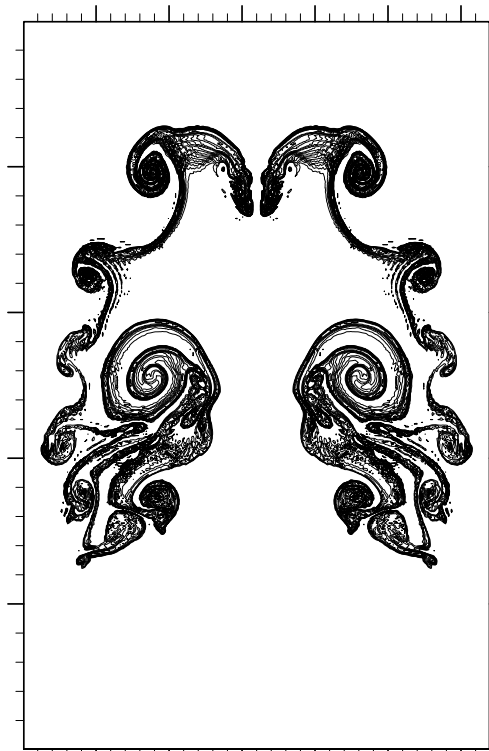
Piecewise parabolic method
Carpenter et al (1990)

Carpenter et al., 1990, Monthly Weather Rev. 118: 586 – 612.

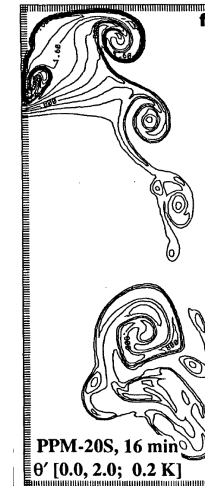
Time = 16.0 min, $dx = 10$ m, comparison of T field



No limiter



van Leer limiter



Piecewise parabolic method
Carpenter et al (1990)

Codes to be compared

NCAR Grabowski: 2nd-order finite difference code with MPDATA (the multidimensional positive definite advection transport), set to constant background density

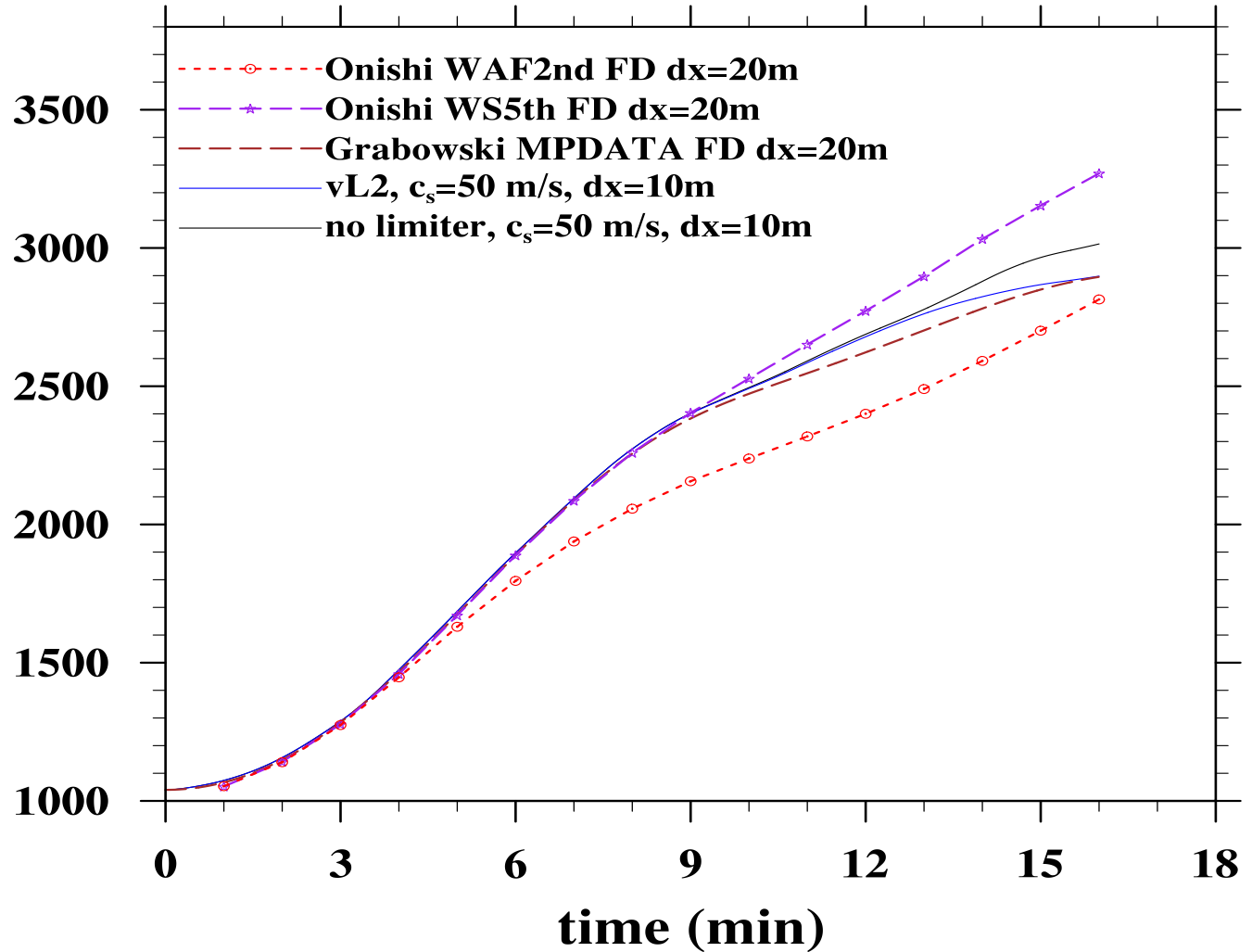
JAMSTec Onishi: atmospheric background density

WAF2nd: 2nd-order Weighted-Averaged Flux method with SUPER-BEE flux limiter

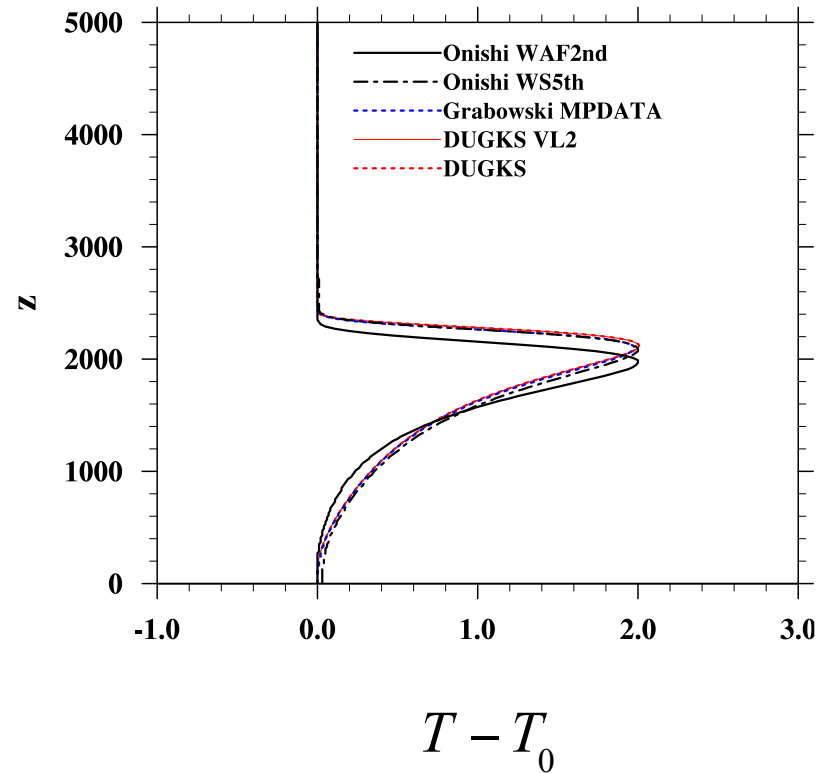
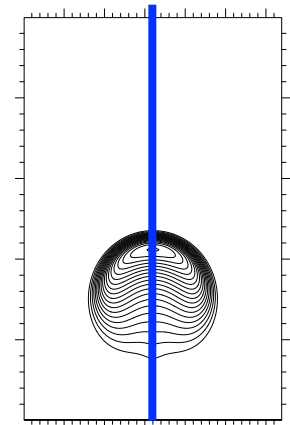
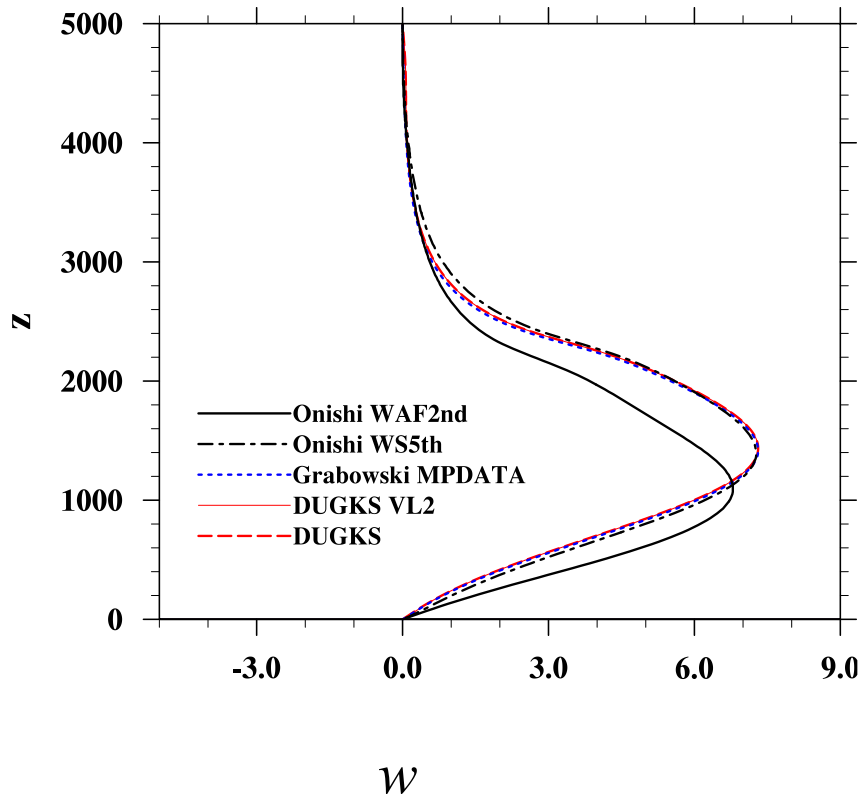
WS5th: Wicker-Skamarock 5th-order upwind scheme

The center of the thermal

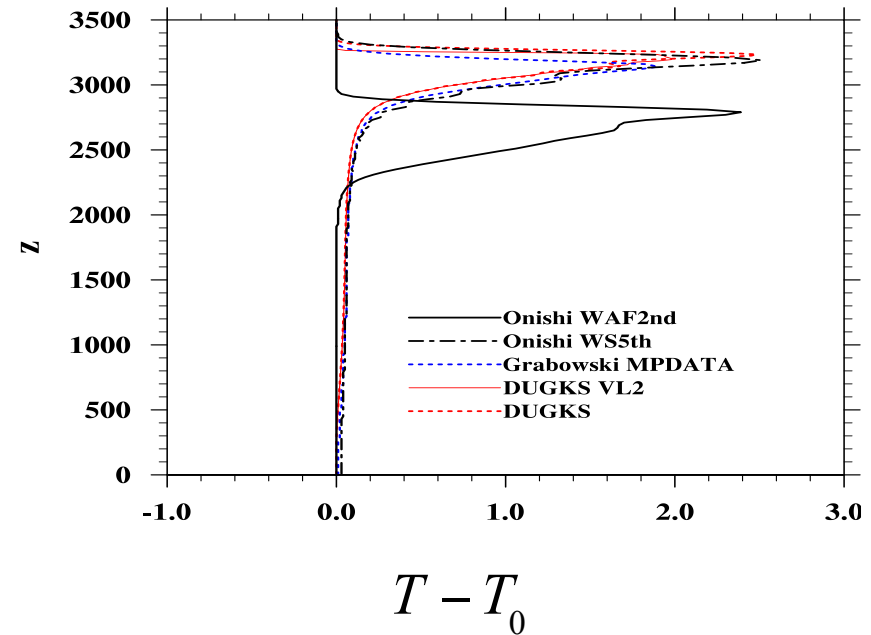
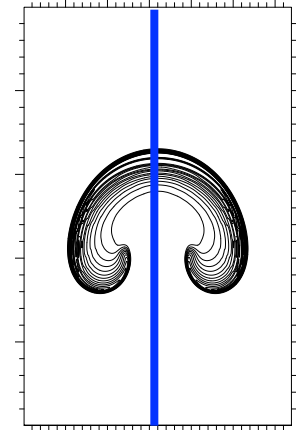
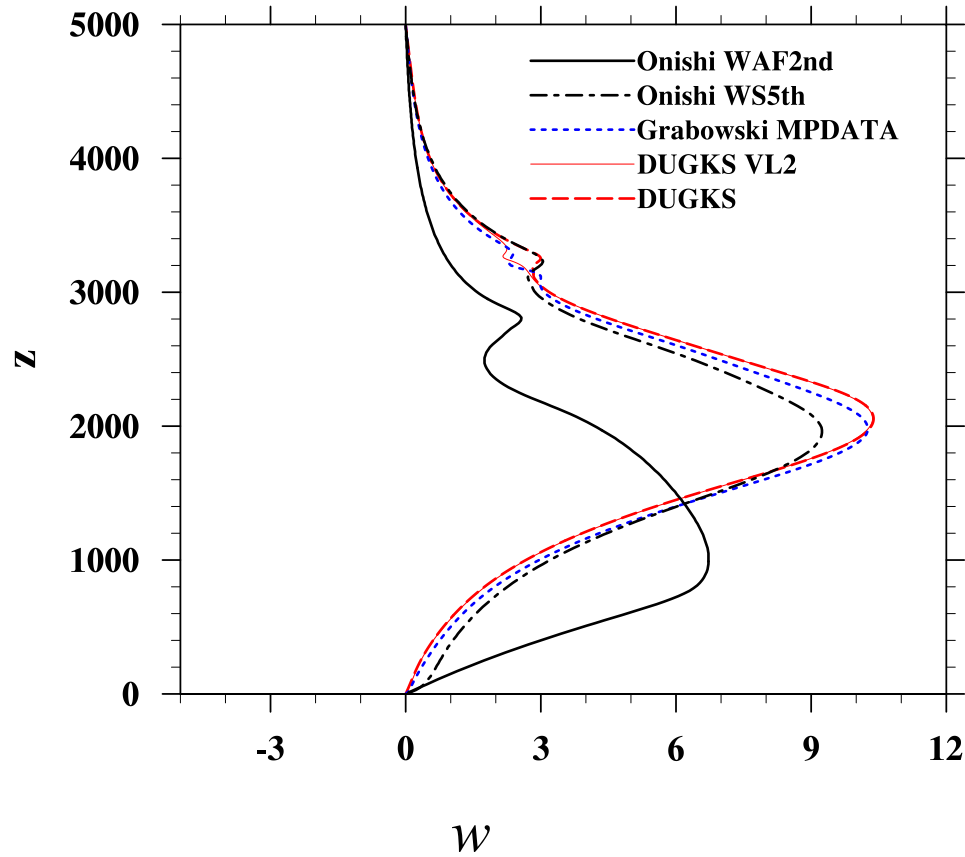
$$Z_c = \frac{\int (\theta - \theta_0) z dV}{\int (\theta - \theta_0) dV}$$



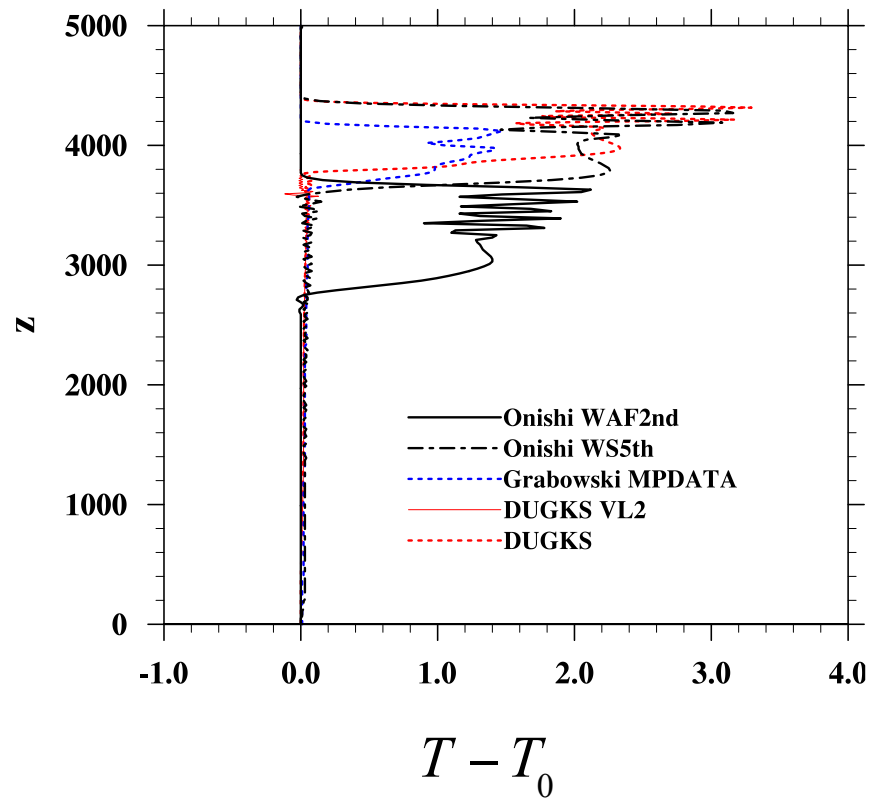
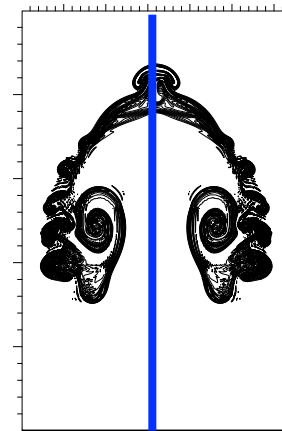
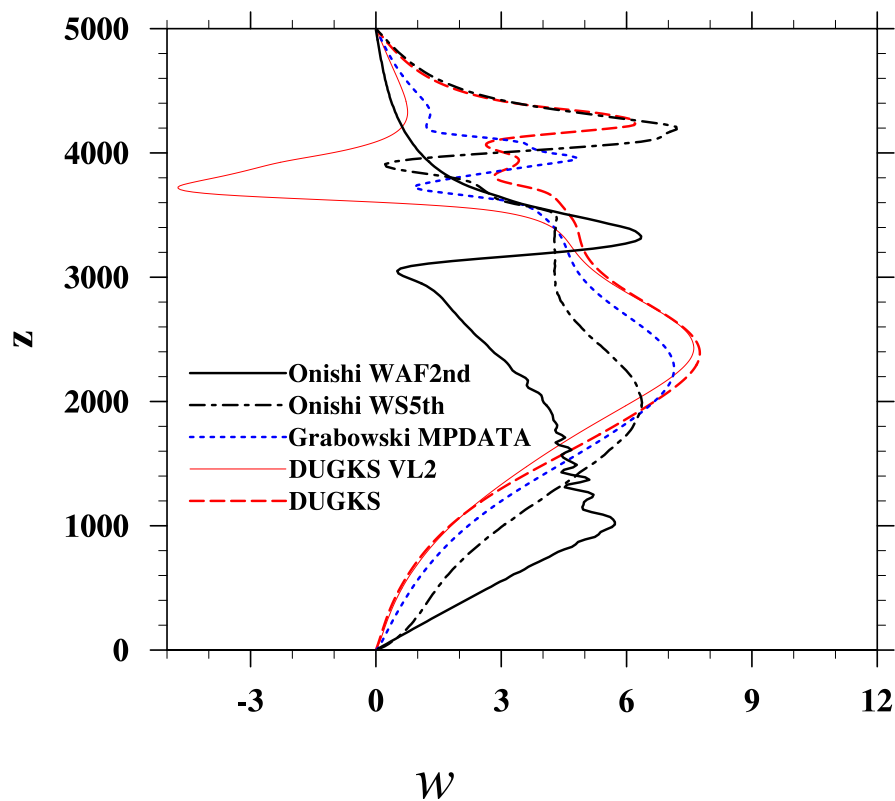
Vertical profiles at 5 min



Vertical profiles at 10 min



Vertical profiles at 15 min



Summary

Demonstrated the feasibility of using DUGKS for high Ra convection flows

- DUGKS has low numerical diffusivity and provides accurate solution for convection flow
- DUGKS code is stable even when the flow is not resolved
- When the flow is unresolved, local oscillations occur
- Numerical limiter help suppress oscillations

At later times, the solution could depend sensitively on the treatment of the advection term, details of the numerical limiter, grid resolution *etc.*, or even how grids are set up relative to the center of the bubble

- How do we develop benchmark solutions at later times?

Potential benefits: fast scalable computation, low numerical dissipation,

Next steps

- Directional splitting may be tested
- Better slope / flux limiter scheme: MPDATA, WENO
- Atmospheric background density / temperature